AIMS Mathematics, 11(11): 37322–37354.
DOI: 10.3934/math.20261444
Received: 16 August 2026
Revised: 16 September 2026
Accepted: 18 September 2026
Published: 11 November 2026

https://www.aimspress.com/journal/Math

Research article

An exponentiated QLindley distribution: properties, inference, and applications

Sajadul Hussain[1], **Partha Jyoti Hazarika**[1], **Ankur Chakraborty**[1] **and Diego I. Gallardo**[2,*]

[1] Department of Statistics, Dibrugarh University, Assam, India

[2] Departamento de Estadística, Facultad de Ciencias, Universidad del Bío-Bío, Concepción, Chile

* **Correspondence:** Email: dgallardo@ubiobio.cl.

Abstract: The exponentiated-G family provides a convenient framework for introducing additional shape parameters into flexible lifetime distributions. In this study, we propose a new two-parameter Exponentiated QLindley (EQL) distribution as an extension of the QLindley model. The proposed distribution exhibits a wide range of density and hazard rate shapes while retaining a tractable parametric structure, with the QLindley distribution obtained as the special case $\alpha = 1$. We derive several mathematical properties of the EQL distribution, including its quantile function, moments, generalized order statistics, reliability characteristics, and actuarial risk measures. We consider both classical and Bayesian estimation methods and conduct a comprehensive Monte Carlo simulation study to investigate their finite-sample performance under different parameter configurations and sample sizes. We illustrate the empirical applicability of the EQL model using four real datasets involving reliability, customer waiting times, air pollution in Delhi, India, and COVID-19 mortality in the Netherlands. We compare the proposed distribution with several well-known competing models using information criteria and goodness-of-fit statistics. The results show that the EQL distribution provides a competitive, flexible alternative for modeling positive, right-skewed data, with the additional shape parameter significantly improving fit relative to the QLindley submodel in all four applications.

Keywords: exponentiated-G family; QLindley distribution; reliability analysis; parameter estimation; Bayesian inference; Monte Carlo simulation
Mathematics Subject Classification: 62E15, 62F10

Supplementray

S1. Additional properties of the EQL distribution

This section presents additional analytical results for the proposed EQL distribution that complement the distributional properties discussed in the main manuscript. Specifically, we provide explicit expressions for moments, incomplete moments and generalized order statistics, including ordinary order statistics and record values.

S1.1. Moments

Proposition S1.1. *Let $X \sim EQL(\alpha, \theta)$. For $r \geq 0$, the r-th ordinary moment $\mu'_r = E(X^r)$ is given by*

$$\begin{aligned}\mu'_r = \frac{\alpha\theta}{1+\theta}\sum_{k=0}^{\infty}(-1)^k\binom{\alpha-1}{k}\sum_{j=0}^{k}\binom{k}{j}\left(\frac{\theta^2}{1+\theta}\right)^j \\ \times\left[\frac{\Gamma(r+j+1)}{[(k+1)\theta]^{r+j+1}} + \theta^2\frac{\Gamma(r+j+2)}{[(k+1)\theta]^{r+j+2}}\right].\end{aligned} \tag{S1.1}$$

Proof. Let $X \sim EQL(\alpha, \theta)$, where $\alpha > 0$ and $\theta > 0$. From the pdf of EQL, the r-th ordinary moment, for $r \geq 0$, is

$$\mu'_r = \int_0^{\infty} x^r f(x; \alpha, \theta)\, dx, \tag{S1.2}$$

and hence

$$\mu'_r = \frac{\alpha\theta}{1+\theta}\int_0^{\infty} x^r(1+\theta^2 x)e^{-\theta x}\,[\mathcal{G}(x;\theta)]^{\alpha-1}\, dx. \tag{S1.3}$$

Define

$$z(x) = \left(1 + \frac{\theta^2 x}{1+\theta}\right)e^{-\theta x}. \tag{S1.4}$$

Then

$$\mathcal{G}(x;\theta) = 1 - z(x). \tag{S1.5}$$

For $x > 0$, we have $0 < z(x) < 1$. Indeed, $z(0) = 1$ and

$$z'(x) = \left[\frac{\theta^2}{1+\theta} - \theta\left(1 + \frac{\theta^2 x}{1+\theta}\right)\right]e^{-\theta x} < 0, \qquad x \geq 0,$$

because

$$\frac{\theta^2}{1+\theta} < \theta.$$

Consequently, $0 < z(x) < 1$ for every $x > 0$.

Therefore, the generalized binomial expansion is valid pointwise for $x > 0$:

$$[1 - z(x)]^{\alpha-1} = \sum_{k=0}^{\infty}(-1)^k\binom{\alpha-1}{k}z(x)^k. \tag{S1.6}$$

For $\alpha = 1, 2, 3, \ldots$, the expansion terminates and the result follows immediately. For non-integer $\alpha > 0$, the expansion is the standard generalized binomial series, which converges absolutely for $|z(x)| < 1$.

We next justify the interchange of summation and integration in (S1.3). Since

$$z(x) \in (0, 1), \qquad x > 0,$$

consider the absolute series

$$\sum_{k=0}^{\infty} \left| \binom{\alpha - 1}{k} \right| z(x)^k. \tag{S1.7}$$

For $\alpha > 1$, the generalized binomial coefficients satisfy

$$\left| \binom{\alpha - 1}{k} \right| = O(k^{-\alpha}), \qquad k \to \infty,$$

so that the series in (S1.7) remains bounded as $z(x) \uparrow 1$. For $0 < \alpha < 1$, the corresponding standard bound is

$$\sum_{k=0}^{\infty} \left| \binom{\alpha - 1}{k} \right| z^k = O\left((1 - z)^{\alpha - 1}\right), \qquad z \uparrow 1.$$

Moreover,

$$1 - z(x) = \mathcal{G}(x; \theta) = \frac{\theta}{1 + \theta} x + O(x^2), \qquad x \downarrow 0.$$

Thus, for $0 < \alpha < 1$,

$$\sum_{k=0}^{\infty} \left| \binom{\alpha - 1}{k} \right| z(x)^k = O(x^{\alpha - 1}), \qquad x \downarrow 0.$$

Consequently, the absolute value of the integrand associated with the series is bounded near zero by a constant multiple of $x^{r+\alpha-1}$, which is integrable because $r \geq 0$ and $\alpha > 0$. As $x \to \infty$, the exponential factor $e^{-\theta x}$ ensures integrability. Hence,

$$\int_0^{\infty} x^r (1 + \theta^2 x) e^{-\theta x} \sum_{k=0}^{\infty} \left| \binom{\alpha - 1}{k} \right| z(x)^k \, dx < \infty. \tag{S1.8}$$

Therefore, by Tonelli's theorem applied to the absolute series (and hence by Fubini's theorem), the order of summation and integration may be interchanged.

Substituting (S1.6) into (S1.3) gives

$$\begin{aligned} \mu_r' &= \frac{\alpha\theta}{1 + \theta} \sum_{k=0}^{\infty} (-1)^k \binom{\alpha - 1}{k} \int_0^{\infty} x^r (1 + \theta^2 x) e^{-\theta x} \left(1 + \frac{\theta^2 x}{1 + \theta}\right)^k e^{-k\theta x} \, dx \\ &= \frac{\alpha\theta}{1 + \theta} \sum_{k=0}^{\infty} (-1)^k \binom{\alpha - 1}{k} \int_0^{\infty} x^r (1 + \theta^2 x) \left(1 + \frac{\theta^2 x}{1 + \theta}\right)^k e^{-(k+1)\theta x} \, dx. \end{aligned} \tag{S1.9}$$

Using the finite binomial expansion

$$\left(1 + \frac{\theta^2 x}{1 + \theta}\right)^k = \sum_{j=0}^{k} \binom{k}{j} \left(\frac{\theta^2}{1 + \theta}\right)^j x^j, \tag{S1.10}$$

we obtain

$$\mu_r' = \frac{\alpha\theta}{1+\theta}\sum_{k=0}^{\infty}(-1)^k\binom{\alpha-1}{k}\sum_{j=0}^{k}\binom{k}{j}\left(\frac{\theta^2}{1+\theta}\right)^j \times \int_0^{\infty} x^{r+j}(1+\theta^2 x)e^{-(k+1)\theta x}\,dx. \tag{S1.11}$$

The remaining integral is evaluated using the gamma-integral identity

$$\int_0^{\infty} x^{a-1}e^{-bx}\,dx = \frac{\Gamma(a)}{b^a}, \qquad a>0, \quad b>0.$$

Thus,

$$\int_0^{\infty} x^{r+j}(1+\theta^2 x)e^{-(k+1)\theta x}\,dx = \frac{\Gamma(r+j+1)}{[(k+1)\theta]^{r+j+1}} + \theta^2\frac{\Gamma(r+j+2)}{[(k+1)\theta]^{r+j+2}}. \tag{S1.12}$$

Substituting (S1.12) into (S1.11) yields Eq (S1.1)

The absolute-integrability argument in (S1.8) also establishes the convergence of the resulting infinite series for all $\alpha > 0$, $\theta > 0$, and $r \geq 0$. For integer $\alpha > 1$, the outer binomial expansion terminates after finitely many terms. Therefore, the moment expression is well defined throughout the parameter space of the EQL distribution. □

Table S1 presents a numerical verification of the raw-moment expression derived in Proposition 2 in the main manuscript. The first three raw moments ($r = 1, 2, 3$) were evaluated for nine representative combinations of the model parameters α and θ, covering different parameter settings. The analytical values obtained from the derived infinite-series expression are compared with the corresponding values calculated by direct numerical integration of the EQL probability density function. An excellent agreement is observed between the two approaches for all considered parameter combinations. The relative errors are very small and decrease substantially for the higher-order moments. The largest relative discrepancy is approximately 2.66×10^{-4}, occurring for the first raw moment at $(\alpha, \theta) = (0.5, 2.5)$, while the relative errors for the second and third moments are considerably smaller. These results provide strong numerical evidence for the accuracy of the derived raw-moment expression and its numerical implementation.

Table S1. Numerical verification of the analytical raw moments of the EQL distribution against direct numerical integration for representative values of (α, θ).

α	θ	r	Analytical	Numerical	Relative error
0.5	0.5	1	1.65380	1.65405	1.55×10^{-4}
0.5	0.5	2	7.31563	7.31563	7.52×10^{-7}
0.5	0.5	3	50.16708	50.16708	4.26×10^{-9}
1.5	0.5	1	3.38762	3.38762	4.03×10^{-7}
1.5	0.5	2	18.48074	18.48074	1.91×10^{-9}
1.5	0.5	3	138.40223	138.40223	1.08×10^{-11}
3.0	0.5	1	4.77709	4.77709	$< 10^{-14}$
3.0	0.5	2	30.70828	30.70828	$< 10^{-14}$
3.0	0.5	3	250.49200	250.49200	$< 10^{-14}$
0.5	1.0	1	0.94146	0.94163	1.81×10^{-4}
0.5	1.0	2	2.21509	2.21509	1.09×10^{-6}
0.5	1.0	3	7.88488	7.88488	7.87×10^{-9}
1.5	1.0	1	1.89000	1.89000	4.81×10^{-7}
1.5	1.0	2	5.50503	5.50503	2.82×10^{-9}
1.5	1.0	3	21.52002	21.52002	2.02×10^{-11}
3.0	1.0	1	2.62731	2.62731	$< 10^{-14}$
3.0	1.0	2	9.01775	9.01775	$< 10^{-14}$
3.0	1.0	3	38.52701	38.52701	$< 10^{-14}$
0.5	2.5	1	0.43983	0.43995	2.66×10^{-4}
0.5	2.5	2	0.43683	0.43683	2.56×10^{-6}
0.5	2.5	3	0.64004	0.64004	2.94×10^{-8}
1.5	2.5	1	0.85242	0.85241	7.31×10^{-7}
1.5	2.5	2	1.05813	1.05813	6.74×10^{-9}
1.5	2.5	3	1.71931	1.71931	7.62×10^{-11}
3.0	2.5	1	1.16023	1.16023	$< 10^{-14}$
3.0	2.5	2	1.69905	1.69905	$< 10^{-14}$
3.0	2.5	3	3.03283	3.03283	$< 10^{-14}$

S1.2. Incomplete moments

The incomplete moments of the EQL distribution are useful for deriving several distributional and reliability-related quantities. In particular, the first incomplete moment is used in the main manuscript to obtain the Bonferroni and Lorenz curves. For $r > -1$, the rth incomplete moment of the EQL distribution is given by

$$\begin{aligned} m_r(t) &= \int_0^t x^r f(x)\, dx \\ &= \frac{\alpha\theta}{1+\theta} \sum_{k=0}^{\infty} (-1)^k \binom{\alpha-1}{k} \sum_{j=0}^{k} \binom{k}{j} \left(\frac{\theta^2}{1+\theta}\right)^j \left[\frac{\gamma(r+j+1, (k+1)\theta t)}{[(k+1)\theta]^{r+j+1}} + \theta^2 \frac{\gamma(r+j+2, (k+1)\theta t)}{[(k+1)\theta]^{r+j+2}} \right], \end{aligned}$$

where $\gamma(\cdot, \cdot)$ is the lower incomplete gamma function.

S1.3. Generalized order statistics

The EQL distribution admits a unified treatment of generalized order statistics (GOS), including ordinary order statistics and record values. The general framework introduced by Kamps [1] is summarized below, followed by the corresponding results for the EQL distribution. Let $X(1,n,m,k),\ldots,X(n,n,m,k)$, where $k \geq 1$ and m is a real number, denote a set of n generalized order statistics (GOS). The joint pdf, denoted by $f_{1,\ldots,n}(x_1,\ldots,x_n)$, is expressed as

$$f_{1,\ldots,n}(x_1,\ldots,x_n) = \begin{cases} k\prod_{j=1}^{n-1}\gamma_j \prod_{i=1}^{n-1}(1-F(x_i))^m f(x_i)\,(1-F(x_n))^{k-1} f(x_n), \\ \qquad F^{-1}(0) < x_1 < \cdots < x_n < F^{-1}(1), \\ 0, \quad \text{otherwise}, \end{cases} \tag{S1.13}$$

where $\gamma_j = k + (n-j)(m+1)$.

For the EQL distribution, substituting $F(x) = [\mathcal{G}(x;\theta)]^\alpha$ and the corresponding density into (S1.13) gives

$$\begin{aligned} f_{1,\ldots,n}(x_1,\ldots,x_n) = k\prod_{j=1}^{n-1}\gamma_j \prod_{i=1}^{n-1}(1-[\mathcal{G}(x_i;\theta)]^\alpha)^m \frac{\alpha\theta(1+\theta^2 x_i)e^{-\theta x_i}}{1+\theta}[\mathcal{G}(x_i;\theta)]^{\alpha-1} \\ \times (1-[\mathcal{G}(x_n;\theta)]^\alpha)^{k-1} \frac{\alpha\theta(1+\theta^2 x_n)e^{-\theta x_n}}{1+\theta}[\mathcal{G}(x_n;\theta)]^{\alpha-1}. \end{aligned}$$

The marginal pdf of the rth generalized order statistic, $X(r,n,m,k)$, is given by

$$f_{r:n,m,k}(x) = \frac{c_r}{(r-1)!}\,[1-F(x)]^{k+(n-r)(m+1)-1}\ f(x)\ \left[g_m(F(x))\right]^{r-1},$$

where $c_r = \prod_{j=1}^{r}\gamma_j$, and

$$g_m(U) = \begin{cases} \dfrac{1}{m+1}\left[1-(1-U)^{m+1}\right], & m \neq -1, \\ -\ln(1-U), & m = -1,\ U \in (0,1). \end{cases}$$

For the EQL distribution, the corresponding marginal pdf is therefore given by

$$f_{r:n,m,k}(x) = \frac{c_r}{(r-1)!}\,[1-[\mathcal{G}(x;\theta)]^\alpha]^{k+(n-r)(m+1)-1}\ \frac{\alpha\theta(1+\theta^2 x)}{1+\theta}e^{-\theta x}\,[\mathcal{G}(x;\theta)]^{\alpha-1}\left[g_m([\mathcal{G}(x;\theta)]^\alpha)\right]^{r-1}, x > 0.$$

Special cases. Several well-known models arise as particular cases of the gos by suitable choices of the parameters m and k:

(1) For $m = 0$ and $k = 1$, Eq (S1.13) reduces to the joint distribution of *ordinary order statistics*.

(2) For $m = -1$, Eq (S1.13) reduces to the joint distribution of the k-th *upper record values*.

(3) For $m = -1$ and $k = 1$, Eq (S1.13) reduces to the joint distribution of *standard upper record values*.

As a special case, consider ordinary order statistics. Let $X_1, \ldots, X_n$ be a random sample from the EQL distribution with parameters α and θ, and let $X_{(1)} \leq \cdots \leq X_{(n)}$ denote the corresponding order statistics. Setting $m = 0$ and $k = 1$ in (S1.13) yields the pdf of the rth order statistic. If we put $m = 0$ and $k = 1$ in (S1.13), we can obtain the pdf of rth order statistic as

$$f_{X_{(r)}}(x) = \frac{n!}{(r-1)!(n-r)!} \frac{\alpha\theta(1+\theta^2 x)}{1+\theta} e^{-\theta x} \left[\mathcal{G}(x;\theta)\right]^{\alpha r-1} \left\{1 - \left[\mathcal{G}(x;\theta)\right]^{\alpha}\right\}^{n-r}, \qquad x > 0.$$

In particular, the density functions of the minimum $X_{(1)}$ and the maximum $X_{(n)}$ are obtained as special cases. For $r = 1$, we have

$$f_{X_{(1)}}(x) = n \, \frac{\alpha\theta(1+\theta^2 x)}{1+\theta} e^{-\theta x} \left[\mathcal{G}(x;\theta)\right]^{\alpha-1} \left\{1 - \left[\mathcal{G}(x;\theta)\right]^{\alpha}\right\}^{n-1}, \qquad x > 0,$$

and for $r = n$, we obtain

$$f_{X_{(n)}}(x) = n \, \frac{\alpha\theta(1+\theta^2 x)}{1+\theta} e^{-\theta x} \left[\mathcal{G}(x;\theta)\right]^{\alpha n-1}, \qquad x > 0.$$

S2. Additional reliability properties

This section presents additional reliability properties of the EQL distribution that complement those discussed in the main manuscript. In particular, we provide explicit expressions for the mean inactivity time, mean residual life, reliability aging intensity, stress–strength reliability, and fuzzy reliability. These results further illustrate the flexibility of the EQL distribution in describing different aging patterns and reliability scenarios.

S2.1. Mean inactivity time function

The mean inactivity time (MIT) function is an important reliability measure with applications in reliability engineering, survival analysis, and actuarial science. It characterizes the expected time that has elapsed since a failure occurred. Using the cdf of the EQL distribution and expanding $\left[1 - (1+\theta^2 x/(1+\theta))e^{-\theta x}\right]^{\alpha}$, we obtain

$$\begin{aligned} \mathrm{MIT}(t) &= E[t - X \mid X \leq t] = \frac{1}{F(t)} \int_0^t F(x)\, dx \\ &= \frac{1}{\left[\mathcal{G}(t;\theta)\right]^{\alpha}} \left[t + \sum_{k=1}^{\infty} (-1)^k \binom{\alpha}{k} \sum_{j=0}^{k} \binom{k}{j} \left(\frac{\theta^2}{1+\theta}\right)^j \frac{\gamma(j+1, k\theta t)}{(k\theta)^{j+1}} \right], \qquad t > 0. \end{aligned}$$

S2.2. Mean residual life function

The mean residual life (MRL) function represents the expected remaining lifetime of a unit conditional on survival up to time t. It is defined by

$$\begin{aligned}\mathrm{MRL}(t) &= E(X-t \mid X>t) = \frac{1}{S(t)}\int_t^{\infty} S(x)\,dx \\ &= \frac{\sum_{k=1}^{\infty}\sum_{j=0}^{k}\binom{\alpha}{k}(-1)^{k+1}\binom{k}{j}\left(\frac{\theta^2}{1+\theta}\right)^j \frac{\Gamma(j+1,\,k\theta t)}{(k\theta)^{j+1}}}{1-[\mathcal{G}(t;\theta)]^{\alpha}}, \qquad t>0,\ \alpha,\theta>0,\end{aligned}$$

where $\Gamma(a,x)$ denotes the upper incomplete gamma function. Numerical evaluations of the MIT and MRL functions under selected parameter configurations are presented in Figure S1. These plots illustrate the sensitivity of the MIT and MRL functions to the parameter values of the EQL distribution.

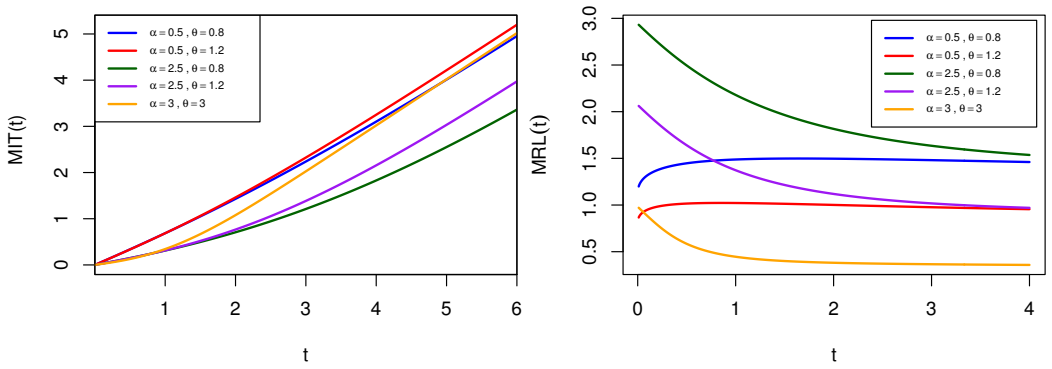


Figure S1. Mean inactivity time and residual life plots of the EQL model with different parameter settings.

S2.3. Reliability aging intensity

The reliability aging intensity (RAI) function is a valuable tool for analyzing the aging behavior of lifetime distributions. It provides a detailed understanding of whether the aging rate of a system increases, decreases, or remains constant over time. The RAI is defined as follows:

$$\mathrm{RAI}(x) = \frac{d}{dx}\log[h(x)] = \frac{\theta^2}{1+\theta^2 x} - \theta + (\alpha-1)\frac{\mathcal{G}'(x;\theta)}{\mathcal{G}(x;\theta)} + \frac{\alpha\,[\mathcal{G}(x;\theta)]^{\alpha-1}\mathcal{G}'(x;\theta)}{1-[\mathcal{G}(x;\theta)]^{\alpha}}, \qquad x>0,$$

where $\mathcal{G}'(x;\theta) = e^{-\theta x}\left[\theta\left(1+\frac{\theta^2 x}{1+\theta}\right) - \frac{\theta^2}{1+\theta}\right]$. Since $h(x)>0$, the sign of $\mathrm{RAI}(x)$ is the same as the sign of $h'(x)$. Therefore, $\mathrm{RAI}(x)<0$ indicates a decreasing failure rate (DFR), whereas $\mathrm{RAI}(x)>0$ indicates an increasing failure rate (IFR).

Table S2 reports numerical values of the hazard rate and the RAI function for selected parameter configurations. For $(\alpha,\theta) = (0.5, 0.5)$, the RAI is negative throughout the range of x considered, indicating a DFR pattern. In contrast, for $(\alpha,\theta) = (2.5, 0.5)$ and $(2.5, 2.0)$, the RAI remains positive over the considered range, indicating an IFR pattern. For $(\alpha,\theta) = (0.5, 2.0)$, the RAI changes sign, indicating a transition from DFR to IFR. These numerical results illustrate the ability of the EQL model to accommodate different aging patterns.

Table S2. Numerical values of the hazard rate, RAI function, and aging classification for the EQL model under selected parameter settings.

	$\alpha = 0.5,\ \theta = 0.5$			$\alpha = 0.5,\ \theta = 2.0$			$\alpha = 2.5,\ \theta = 0.5$			$\alpha = 2.5,\ \theta = 2.0$		
x	$h(x)$	RAI(x)	Type	$h(x)$	RAI(x)	Type	$h(x)$	RAI(x)	Type	$h(x)$	RAI(x)	Type
0.10	1.09419	-4.09865	DFR	1.94520	-2.49651	DFR	0.00485	14.55900	IFR	0.03704	16.79073	IFR
0.25	0.76831	-1.43212	DFR	1.64320	-0.47060	DFR	0.01796	5.56042	IFR	0.17190	6.51330	IFR
0.50	0.61086	-0.60118	DFR	1.56465	-0.05293	DFR	0.04556	2.57058	IFR	0.48804	2.67413	IFR
1.00	0.50882	-0.22336	DFR	1.57781	0.04815	IFR	0.10473	1.10126	IFR	1.04168	0.83066	IFR
2.00	0.45018	-0.06366	DFR	1.66530	0.05084	IFR	0.20527	0.41347	IFR	1.55159	0.17274	IFR
3.00	0.43283	-0.02213	DFR	1.73875	0.03557	IFR	0.27636	0.21267	IFR	1.71714	0.05746	IFR

S2.4. Fuzzy reliability

Fuzzy reliability provides a framework for incorporating uncertainty in the definition of a survival threshold. Let $X \sim \text{EQL}(\alpha, \theta)$ and consider a fuzzy lifetime requirement characterized by the interval $[\zeta_1, \zeta_2]$, where $0 \le \zeta_1 < \zeta_2$. The associated membership function is defined as

$$\vartheta(y) = \begin{cases} 0, & y \le \zeta_1, \\ \dfrac{y - \zeta_1}{\zeta_2 - \zeta_1}, & \zeta_1 < y < \zeta_2, \\ 1, & y \ge \zeta_2. \end{cases}$$

Thus, values below ζ_1 do not satisfy the lifetime requirement, whereas values above ζ_2 fully satisfy it, with a gradual transition between these two limits.

For a confidence level $L \in [0, 1]$, the corresponding L-cut is represented by the threshold

$$y(L) = \zeta_1 + L(\zeta_2 - \zeta_1), \qquad 0 \le L \le 1. \tag{S2.1}$$

In particular, $y(0) = \zeta_1$ and $y(1) = \zeta_2$. Following the fuzzy reliability formulation adopted here, the reliability measure associated with the L-cut can be expressed in terms of the survival function as

$$R_F(L) = S(\zeta_1; \alpha, \theta) - S(y(L); \alpha, \theta). \tag{S2.2}$$

Hence, $R_F(L)$ measures the probability mass accumulated between ζ_1 and the L-cut threshold $y(L)$, and satisfies

$$R_F(0) = 0, \qquad R_F(1) = S(\zeta_1; \alpha, \theta) - S(\zeta_2; \alpha, \theta).$$

Because the survival function is decreasing, $R_F(L)$ is nondecreasing in L. For the EQL distribution, Eq (S2.2) becomes

$$\begin{aligned} R_F(L) &= \left[1 - \left\{1 - \left(1 + \frac{\theta^2 \zeta_1}{1+\theta}\right) e^{-\theta\zeta_1}\right\}^{\alpha}\right] - \left[1 - \left\{1 - \left(1 + \frac{\theta^2 y(L)}{1+\theta}\right) e^{-\theta y(L)}\right\}^{\alpha}\right] \\ &= \left\{1 - \left(1 + \frac{\theta^2 y(L)}{1+\theta}\right) e^{-\theta y(L)}\right\}^{\alpha} - \left\{1 - \left(1 + \frac{\theta^2 \zeta_1}{1+\theta}\right) e^{-\theta\zeta_1}\right\}^{\alpha}, \end{aligned}$$

where $y(L)$ is given by Eq (S2.1). The classical reliability at a fixed threshold y is given by the survival function $S(y;\alpha,\theta)$. In contrast, $R_F(L)$ provides a threshold-dependent assessment over the interval $[\zeta_1,\zeta_2]$ and represents the probability mass accumulated between ζ_1 and the L-cut threshold $y(L)$. A numerical illustration of the fuzzy reliability measure for selected values of $(\alpha,\theta,\zeta_1,\zeta_2)$ and L is provided in Table S3. The corresponding computations are summarized in Algorithm 1.

Table S3. Fuzzy reliability of the EQL model for different values of α, θ, ζ_1, ζ_2 and L.

α	θ	ζ_1	ζ_2	$S(\zeta_1)$	$S(\zeta_2)$	$R_F(L=0.25)$	$R_F(L=0.5)$	$R_F(L=0.75)$
1.5	0.2	0.05	1.0	0.9992438	0.9395789	0.0093780	0.0235545	0.0406154
2.0	0.4	0.10	1.5	0.9992031	0.8724750	0.0140317	0.0422428	0.0808548
2.5	0.8	0.20	2.0	0.9977508	0.6534002	0.0349606	0.1141172	0.2232479
3.0	1.0	0.30	2.5	0.9967543	0.4580411	0.0565004	0.1926598	0.3684628
4.0	1.5	0.50	3.0	0.9901458	0.1545512	0.1454122	0.4280319	0.6789025

Algorithm 1. Computation of the fuzzy reliability for the EQL model

1: **Input:** Parameters (α,θ), interval (ζ_1,ζ_2), and L-cut level $L\in[0,1]$.

2: Compute

$$y(L)=\zeta_1+L(\zeta_2-\zeta_1).$$

3: Compute

$$S(\zeta_1;\alpha,\theta)=\left[1-\left(1+\frac{\theta^2\zeta_1}{1+\theta}\right)e^{-\theta\zeta_1}\right]^{\alpha}.$$

4: Compute

$$S(y(L);\alpha,\theta)=\left[1-\left(1+\frac{\theta^2 y(L)}{1+\theta}\right)e^{-\theta y(L)}\right]^{\alpha}.$$

5: Compute

$$R_F(L)=S(\zeta_1;\alpha,\theta)-S(y(L);\alpha,\theta).$$

6: **Return** $R_F(L)$.

Table S3 presents the numerical values of the fuzzy reliability of the proposed model. The following observations are based on the results of the comparative analysis:

- For all parameter configurations, the fuzzy reliability $R_F(L)$ increases monotonically with L, as expected from the monotonicity of the survival function.
- The survival probabilities satisfy $S(\zeta_1)>S(\zeta_2)$ in every case, confirming the decreasing nature of the EQL survival function and the consistency of the numerical results.
- The magnitude of $R_F(L)$ varies substantially across the considered parameter configurations and uncertainty intervals, illustrating the sensitivity of the fuzzy reliability measure to both the EQL parameters and the specification of the threshold interval.

S3. Entropy measures

Entropy measures provide quantitative assessments of the uncertainty associated with a probability distribution. In this section, we present additional entropy results for the EQL distribution, focusing on the Rényi and Shannon entropies. We derive the corresponding analytical expressions and provide numerical evaluations for selected parameter configurations.

S3.1. Rényi entropy

The Rényi entropy of order q, for $q > 0$ and $q \neq 1$, is defined by

$$\mathcal{H}_q(X) = \frac{1}{1-q} \log \left\{ \int_0^\infty f(x)^q \, dx \right\}.$$

The Rényi entropy for the EQL model can be expressed as

$$\begin{aligned} \mathcal{H}_q &= \frac{1}{1-q} \log\left(\int_0^\infty f(x)^q \, dx \right). \\ &= \frac{1}{1-q} \log\left[\left(\frac{\alpha\theta}{1+\theta} \right)^q \sum_{k=0}^{\infty} \binom{q(\alpha-1)}{k} (-1)^k \sum_{i=0}^{\infty} \sum_{j=0}^{k} \binom{q}{i} \binom{k}{j} \theta^{2i} \left(\frac{\theta^2}{1+\theta} \right)^j \frac{\Gamma(i+j+1)}{[(q+k)\theta]^{i+j+1}} \right], \end{aligned}$$

where $\binom{a}{b} = a(a-1)\cdots(a-b+1)/b!$ denotes the generalized binomial coefficient. Table S4 reports numerical values of the Rényi and Shannon entropies for selected combinations of α and θ. For the parameter configurations considered, the Rényi entropy decreases as q increases. These numerical results illustrate how the entropy measure varies with the order q and with the model parameters.

Table S4. Shannon and Rényi entropy values of the EQL model for selected parameter combinations.

Parameters		Shannon	Rényi entropy				
α	θ	H	$q = 0.5$	$q = 1.5$	$q = 2$	$q = 2.5$	$q = 3$
0.8	0.5	1.8271115	2.2303783	1.6054800	1.4482231	1.3203690	1.2053018
1.5	1.5	1.1850911	1.4372787	1.0711964	1.0030749	0.9566185	0.9224113
2.0	0.5	2.2430622	2.5031307	2.1249605	2.0542138	2.0059786	1.9704963
3.0	0.8	1.8831139	2.1291288	1.7699046	1.7015010	1.6546014	1.6199684
5.0	3.0	0.6326254	0.8782719	0.5189215	0.4501222	0.4029348	0.3680887
0.8	1.5	0.9220532	1.2596231	0.7498866	0.6344092	0.5442487	0.4648469

S3.2. Shannon entropy

As $q \to 1$, the Rényi entropy converges to the Shannon entropy. Using the representation of the EQL density and expanding $\log \mathcal{G}(X;\theta)$ in a convergent series, the Shannon entropy can be expressed as

$$
\begin{aligned}
H &= -\int_0^{\infty} f(x)\,\log f(x)\,dx \\
&= -\log\!\left(\frac{\alpha\theta}{1+\theta}\right) - E\Big[\log(1+\theta^2 X)\Big] + \theta\,E[X] \\
&\quad + (\alpha-1)\sum_{m=1}^{\infty}\frac{1}{m}\,\frac{\alpha\theta}{1+\theta}\sum_{k=0}^{\infty}(-1)^k\binom{\alpha-1}{k}\sum_{j=0}^{k+m}\binom{k+m}{j}\left(\frac{\theta^2}{1+\theta}\right)^j \\
&\quad \times\left[\frac{\Gamma(j+1)}{[(k+m+1)\theta]^{j+1}} + \theta^2\frac{\Gamma(j+2)}{[(k+m+1)\theta]^{j+2}}\right].
\end{aligned}
$$

Figure S2 illustrates the behavior of the Rényi entropy $\mathcal{H}_q(X)$ for different parameter configurations. The Rényi entropy decreases with q for the parameter settings considered, and its limiting value at $q = 1$ agrees with the corresponding Shannon entropy. These results provide a numerical verification of the consistency between the two entropy measures.

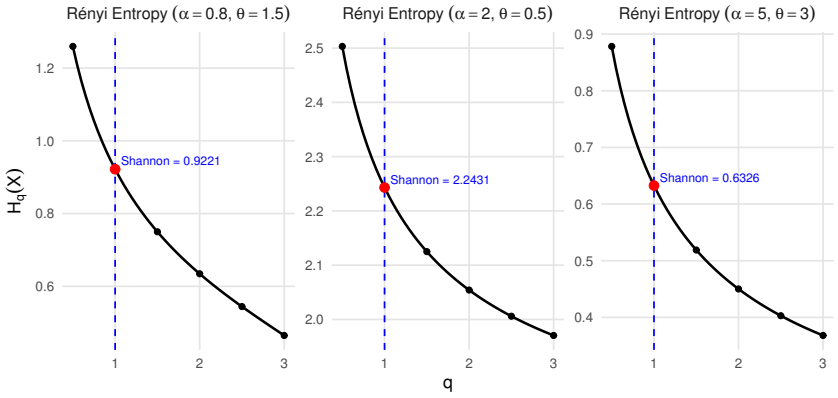


Figure S2. Rényi entropy $\mathcal{H}_q(X)$ of the EQL model for selected parameter combinations (α, θ). The vertical dashed line indicates $q = 1$, corresponding to the Shannon entropy limit.

S4. Actuarial measures

This section presents several actuarial risk measures for the EQL distribution, including the limited expected value (LEV), value-at-risk (VaR), tail value-at-risk (TVaR), tail variance (TV), and expected shortfall (ES). Closed-form or series representations are derived for these measures whenever available.

S4.1. Limited expected value function

The limited expected value (LEV) is a fundamental actuarial measure that quantifies the expected value of a loss variable when the payment is capped at a threshold t. For a nonnegative random variable X, it is defined as

$$
X \wedge t = \min(X, t) = \begin{cases} X, & X \le t, \\ t, & X > t. \end{cases}
$$

Thus, the LEV function can be expressed as

$$\begin{aligned}\mathrm{LEV}(t) = E(X \wedge t) &= \int_0^t x f(x)\,dx + tS(t) \\ &= \int_0^t S(x)\,dx = t - \sum_{k=1}^{\infty} \binom{\alpha}{k} (-1)^k \sum_{j=0}^{k} \binom{k}{j} \left(\frac{\theta^2}{1+\theta}\right)^j \frac{\gamma(j+1, k\theta t)}{(k\theta)^{j+1}}, \qquad t > 0,\end{aligned}$$

where $\gamma(a, x)$ denotes the lower incomplete gamma function.

S4.2. Value-at-risk and tail value-at-risk

The value-at-risk (VaR) is a widely used actuarial and financial risk measure that quantifies the loss threshold exceeded with probability $1 - p$. For the EQL distribution, the VaR at probability level $p \in (0, 1)$ is obtained from the quantile function as

$$\mathrm{VaR}_p = F^{-1}(p).$$

Using the quantile function of the EQL distribution, we obtain

$$\mathrm{VaR}_p = -\frac{1+\theta}{\theta^2} - \frac{1}{\theta} W_{-1}\left[-\frac{1+\theta}{\theta}\left(1 - p^{1/\alpha}\right) e^{-(1+\theta)/\theta}\right], \qquad 0 < p < 1,$$

where $W_{-1}(\cdot)$ denotes the lower real branch of the Lambert W function. The tail value-at-risk (TVaR), also known as the conditional tail expectation, is defined by

$$\mathrm{TVaR}_p = E[X \mid X > \mathrm{VaR}_p] = \frac{1}{1-p} \int_{\mathrm{VaR}_p}^{\infty} x f(x)\,dx.$$

Equivalently,

$$\begin{aligned}\mathrm{TVaR}_p &= \mathrm{VaR}_p + \frac{1}{1-p} \int_{\mathrm{VaR}_p}^{\infty} S(x)\,dx \\ &= \mathrm{VaR}_p + \frac{1}{1-p} \sum_{k=1}^{\infty} \binom{\alpha}{k} (-1)^{k+1} \sum_{j=0}^{k} \binom{k}{j} \left(\frac{\theta^2}{1+\theta}\right)^j \frac{\Gamma\left(j+1, k\theta \mathrm{VaR}_p\right)}{(k\theta)^{j+1}},\end{aligned}$$

where $\Gamma(a, x)$ denotes the upper incomplete gamma function.

S4.3. Tail variance and expected shortfall

The tail variance (TV) measures the conditional variability of the loss distribution beyond the VaR threshold. For the EQL distribution, it is defined as

$$\begin{aligned}\mathrm{TV}_p &= \mathrm{Var}(X \mid X > \mathrm{VaR}_p) \\ &= E[X^2 \mid X > \mathrm{VaR}_p] - \left(\mathrm{TVaR}_p\right)^2 \\ &= \frac{1}{1-p} \int_{\mathrm{VaR}_p}^{\infty} x^2 f(x)\,dx - \left(\mathrm{TVaR}_p\right)^2 \\ &= (\mathrm{VaR}_p)^2 + \frac{2}{1-p} \sum_{k=1}^{\infty} \binom{\alpha}{k} (-1)^{k+1} \sum_{j=0}^{k} \binom{k}{j} \left(\frac{\theta^2}{1+\theta}\right)^j \frac{\Gamma\left(j+2, k\theta \mathrm{VaR}_p\right)}{(k\theta)^{j+2}} - \left(\mathrm{TVaR}_p\right)^2.\end{aligned}$$

The numerical values and some graphical presentation of the main risk measures for the EQL model is examined in this section. It is important to note that a model with larger values of these risk measures is interpreted as having a heavier tail. The numerical results for the VaR, TVaR, TV and ES of the EQL model are reported in Table S5, while the graphical representation of VaR and TVaR are shwon in Figure S3.

Table S5. Numerical values of VaR_p, TVaR_p, TV_p and ES_p for the EQL model.

	$\alpha = 0.5, \theta = 0.2$				$\alpha = 0.5, \theta = 1.0$			
p	VaR_p	TVaR_p	TV_p	ES_p	VaR_p	TVaR_p	TV_p	ES_p
0.75	4.8881	10.2177	29.6470	1.3811	1.3393	2.5528	1.4185	0.4046
0.80	6.0231	11.4142	29.8737	1.6343	1.6131	2.8233	1.4059	0.4712
0.85	7.5293	12.9733	30.0451	1.9344	1.9667	3.1706	1.3885	0.5483
0.90	9.7051	15.1901	30.1304	2.3014	2.4635	3.6565	1.3641	0.6400
0.95	13.4970	19.0013	30.0405	2.7791	3.3030	4.4768	1.3251	0.7556
0.99	22.3710	27.8346	29.4726	3.3454	5.1976	6.3337	1.2556	0.8872
	$\alpha = 2.5, \theta = 0.2$				$\alpha = 2.5, \theta = 1.0$			
0.75	12.8822	18.7050	31.7411	6.7635	3.1686	4.4129	1.4037	1.7652
0.80	14.2454	19.9959	31.3052	7.1871	3.4659	4.6880	1.3744	1.8619
0.85	15.9609	21.6394	30.8548	7.6505	3.8366	5.0361	1.3438	1.9667
0.90	18.3217	23.9259	30.3668	8.1736	4.3416	5.5175	1.3101	2.0837
0.95	22.2587	27.7791	29.7763	8.7999	5.1740	6.3222	1.2681	2.2221
0.99	31.1532	36.5701	28.9641	9.4779	7.0253	8.1379	1.2101	2.3694

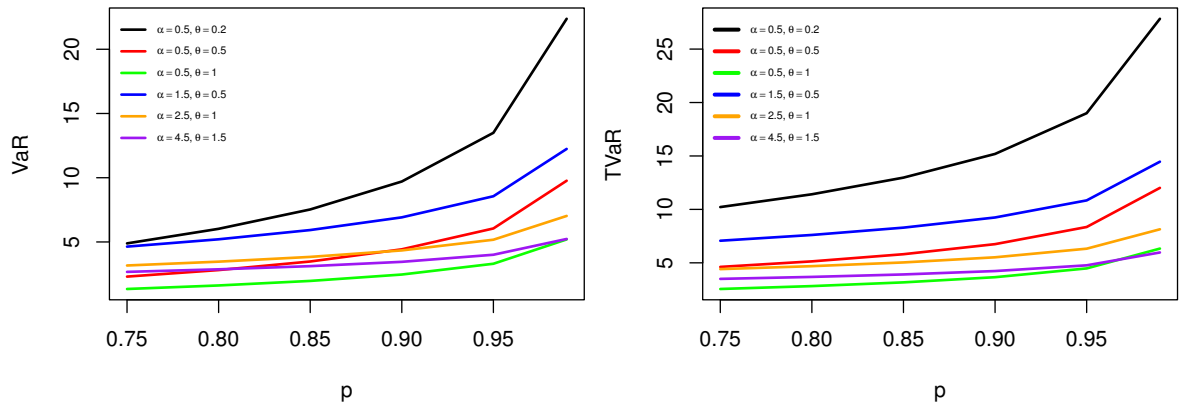


Figure S3. Plots of VaR and TVaR of EQL model.

S5. Additional estimation procedures

In addition to maximum likelihood estimation, we consider several alternative estimation and inferential procedures for the EQL distribution. These include spacing-based and minimum-distance estimation methods, resampling-based confidence intervals, and Bayesian inference.

S5.1. Alternative estimation methods

In addition to maximum likelihood estimation, we consider several alternative estimation procedures for the EQL distribution. These methods are based on probability spacings and minimum-distance criteria and provide useful alternatives when likelihood-based estimation is computationally challenging or sensitive to numerical optimization. Specifically, we consider the Maximum Product Spacing (MPS), Ordinary Least Squares (OLS), Weighted Least Squares (WLS), Cramér–von Mises (CvM), Anderson–Darling (AD), and Minimum Spacing Absolute Distance (MSAD) methods (see for more details [2]).

S5.1.1. Method of Maximum Product Spacing

The Maximum Product Spacing (MPS) method provides an alternative to maximum likelihood estimation, particularly when the likelihood function may present numerical difficulties. Let $x_{1:n} \leq \cdots \leq x_{n:n}$ denote the ordered observations, and define the spacings

$$D_i(\alpha, \theta) = F(x_{i:n}; \alpha, \theta) - F(x_{i-1:n}; \alpha, \theta), \qquad i = 1, \ldots, n+1,$$

where $x_{0:n} = 0$ and $x_{n+1:n} = \infty$. Thus,

$$D_1(\alpha, \theta) = F(x_{1:n}; \alpha, \theta), \qquad D_{n+1}(\alpha, \theta) = 1 - F(x_{n:n}; \alpha, \theta).$$

The MPS estimators $(\widehat{\alpha}_{\mathrm{MPS}}, \widehat{\theta}_{\mathrm{MPS}})$ are obtained by maximizing the geometric mean of these spacings, equivalently,

$$H(\alpha, \theta) = \left\{ \prod_{i=1}^{n+1} D_i(\alpha, \theta) \right\}^{1/(n+1)}.$$

For the EQL distribution, the spacings are computed using $F(x; \alpha, \theta) = [\mathcal{G}(x; \theta)]^{\alpha}$.

S5.1.2. Method of Ordinary and Weighted Least Squares

The Ordinary Least Squares (OLS) and Weighted Least Squares (WLS) methods estimate the model parameters by minimizing discrepancies between the fitted distribution function evaluated at the ordered observations and the corresponding expected values of uniform order statistics. For the EQL distribution, the OLS estimators are obtained by minimizing

$$\mathcal{S}_{\mathrm{OLS}}(\alpha, \theta) = \sum_{i=1}^{n} \left[[\mathcal{G}(x_{i:n}; \theta)]^{\alpha} - \frac{i}{n+1} \right]^2. \tag{S5.1}$$

The WLS method assigns larger weights to observations located near the tails of the distribution. Its objective function is given by

$$\mathcal{S}_{\mathrm{WLS}}(\alpha, \theta) = \sum_{i=1}^{n} \frac{(n+1)^2(n+2)}{i(n+1-i)} \left[[\mathcal{G}(x_{i:n}; \theta)]^{\alpha} - \frac{i}{n+1} \right]^2. \tag{S5.2}$$

The corresponding OLS and WLS estimators are obtained by minimizing (S5.1) and (S5.2), respectively, over $(\alpha, \theta) \in (0, \infty)^2$.

S5.1.3. Method of Cramér–von Mises

The Cramér–von Mises (CvM) method is a minimum-distance estimation procedure that determines the parameter values by minimizing the squared discrepancy between the fitted distribution function and the expected values of the empirical distribution function at the ordered observations. For the EQL distribution, the corresponding objective function is

$$C_{\mathrm{CvM}}(\alpha,\theta)=\frac{1}{12n}+\sum_{i=1}^{n}\left[[\mathcal{G}(x_{i:n};\theta)]^{\alpha}-\frac{2i-1}{2n}\right]^2.$$

The CvM estimators $(\widehat{\alpha}_{\mathrm{CvM}},\widehat{\theta}_{\mathrm{CvM}})$ are obtained by minimizing $C_{\mathrm{CvM}}(\alpha,\theta)$ over $(\alpha,\theta)\in(0,\infty)^2$.

S5.1.4. Method of Anderson–Darling

The Anderson–Darling (AD) method is another minimum-distance estimation procedure that places greater emphasis on discrepancies occurring in the tails of the distribution. This feature makes it particularly useful when accurate characterization of extreme observations is of interest. For the EQL distribution, the AD objective function is given by

$$A_{\mathrm{AD}}(\alpha,\theta)=-n-\frac{1}{n}\sum_{i=1}^{n}(2i-1)\Big\{\log\left([\mathcal{G}(x_{i:n};\theta)]^{\alpha}\right)+\log\left[1-[\mathcal{G}(x_{n+1-i:n};\theta)]^{\alpha}\right]\Big\}.$$

The AD estimators $(\widehat{\alpha}_{\mathrm{AD}},\widehat{\theta}_{\mathrm{AD}})$ are obtained by minimizing $A_{\mathrm{AD}}(\alpha,\theta)$ over $(\alpha,\theta)\in(0,\infty)^2$.

S5.1.5. Method of Minimum Spacing Absolute Distance

The Minimum Spacing Absolute Distance (MSAD) method, introduced by Torabi [3], is an alternative spacing-based estimation procedure for continuous probability distributions. Unlike the MPS method, which maximizes the product of the probability spacings, MSAD estimates the unknown parameters by minimizing the sum of the absolute deviations of the observed probability spacings from their expected value. Define

$$D_i(\alpha,\theta)=F(x_{i:n};\alpha,\theta)-F(x_{i-1:n};\alpha,\theta),\qquad i=1,\ldots,n+1.$$

The MSAD objective function for the EQL distribution is then defined as

$$D_{\mathrm{MSAD}}(\alpha,\theta)=\sum_{i=1}^{n+1}\left|D_i(\alpha,\theta)-\frac{1}{n+1}\right|.$$

The MSAD estimators $(\widehat{\alpha}_{\mathrm{MSAD}},\widehat{\theta}_{\mathrm{MSAD}})$ are obtained by minimizing $D_{\mathrm{MSAD}}(\alpha,\theta)$ over $(\alpha,\theta)\in(0,\infty)^2$.

S5.2. Resampling-based confidence intervals

In this study, bootstrap confidence intervals are constructed for the maximum likelihood estimators $(\widehat{\alpha},\widehat{\theta})$. Let $\mathbf{x}=(x_1,\ldots,x_n)$ denote the observed sample, and let $\mathbf{x}^{*(k)}=(x_1^{*(k)},\ldots,x_n^{*(k)})$ denote the kth bootstrap sample obtained by sampling with replacement from $\mathbf{x}$, for $k=1,\ldots,K$. For each bootstrap

sample, the maximum likelihood estimators $(\widehat{\alpha}^{*(k)}, \widehat{\theta}^{*(k)})$ are obtained by maximizing the likelihood function of the EQL distribution.

For a generic parameter $\psi \in \{\alpha, \theta\}$, let $\widehat{\psi}^{*(1)}, \ldots, \widehat{\psi}^{*(K)}$ denote the corresponding bootstrap estimates. The bootstrap mean and standard error are given by

$$\bar{\psi}^* = \frac{1}{K}\sum_{k=1}^{K}\widehat{\psi}^{*(k)} \qquad \text{and} \qquad \widehat{\mathrm{SE}}_{\mathrm{boot}}(\widehat{\psi}) = \left[\frac{1}{K-1}\sum_{k=1}^{K}\left(\widehat{\psi}^{*(k)} - \bar{\psi}^*\right)^2\right]^{1/2},$$

respectively. Four bootstrap confidence interval procedures are considered: the Normal, Basic, Percentile, and Bias-Corrected and Accelerated (BCa) intervals. Let $1-\gamma$ denote the desired confidence level and let $\widehat{\psi}^*_{(q)}$ denote the empirical qth quantile of the bootstrap estimates. The Normal bootstrap confidence interval is

$$\widehat{\psi} \pm z_{1-\gamma/2}\widehat{\mathrm{SE}}_{\mathrm{boot}}(\widehat{\psi}),$$

where $z_{1-\gamma/2}$ denotes the $(1-\gamma/2)$th quantile of the standard normal distribution. The Basic bootstrap confidence interval is

$$\left(2\widehat{\psi} - \widehat{\psi}^*_{(1-\gamma/2)},\ 2\widehat{\psi} - \widehat{\psi}^*_{(\gamma/2)}\right),$$

whereas the Percentile bootstrap confidence interval is

$$\left(\widehat{\psi}^*_{(\gamma/2)},\ \widehat{\psi}^*_{(1-\gamma/2)}\right).$$

The BCa interval additionally accounts for both bias and skewness in the bootstrap distribution. Let z_0 denote the bias-correction constant and a the acceleration constant. Define

$$q_L = \Phi\left[z_0 + \frac{z_0 + z_{\gamma/2}}{1 - a(z_0 + z_{\gamma/2})}\right] \qquad \text{and} \qquad q_U = \Phi\left[z_0 + \frac{z_0 + z_{1-\gamma/2}}{1 - a(z_0 + z_{1-\gamma/2})}\right],$$

where $\Phi(\cdot)$ is the standard normal cumulative distribution function. The resulting BCa confidence interval is

$$\left(\widehat{\psi}^*_{(q_L)},\ \widehat{\psi}^*_{(q_U)}\right).$$

The four confidence intervals are obtained separately for $\psi = \alpha$ and $\psi = \theta$. The complete bootstrap procedure is summarized in Algorithm 2.

Algorithm 2. Bootstrap-based confidence intervals for the parameters (α, θ) of the EQL distribution.

Input: Sample $\mathbf{x} = (x_1, \ldots, x_n)$, number of bootstrap samples K, and significance level γ.
Output: Normal, Basic, Percentile, and BCa confidence intervals for (α, θ).

for $k = 1$ **to** K **do**
Draw a bootstrap sample $\mathbf{x}^{*(k)}$ of size n with replacement from $\mathbf{x}$;
Compute $(\widehat{\alpha}^{*(k)}, \widehat{\theta}^{*(k)})$ by maximum likelihood estimation;
end for

Compute the bootstrap means:

$$\bar{\alpha}^* = \frac{1}{K}\sum_{k=1}^{K}\widehat{\alpha}^{*(k)}, \qquad \bar{\theta}^* = \frac{1}{K}\sum_{k=1}^{K}\widehat{\theta}^{*(k)}.$$

Compute the bootstrap standard errors:

$$\widehat{\mathrm{SE}}_{\mathrm{boot}}(\widehat{\alpha}) = \left[\frac{1}{K-1}\sum_{k=1}^{K}\left(\widehat{\alpha}^{*(k)} - \bar{\alpha}^*\right)^2\right]^{1/2},$$

$$\widehat{\mathrm{SE}}_{\mathrm{boot}}(\widehat{\theta}) = \left[\frac{1}{K-1}\sum_{k=1}^{K}\left(\widehat{\theta}^{*(k)} - \bar{\theta}^*\right)^2\right]^{1/2}.$$

Normal CI:

$$\widehat{\alpha} \pm z_{1-\gamma/2}\widehat{\mathrm{SE}}_{\mathrm{boot}}(\widehat{\alpha}), \qquad \widehat{\theta} \pm z_{1-\gamma/2}\widehat{\mathrm{SE}}_{\mathrm{boot}}(\widehat{\theta}).$$

Basic CI:

$$\left(2\widehat{\alpha} - \widehat{\alpha}^*_{(1-\gamma/2)},\ 2\widehat{\alpha} - \widehat{\alpha}^*_{(\gamma/2)}\right),$$
$$\left(2\widehat{\theta} - \widehat{\theta}^*_{(1-\gamma/2)},\ 2\widehat{\theta} - \widehat{\theta}^*_{(\gamma/2)}\right).$$

Percentile CI:

$$\left(\widehat{\alpha}^*_{(\gamma/2)},\ \widehat{\alpha}^*_{(1-\gamma/2)}\right), \qquad \left(\widehat{\theta}^*_{(\gamma/2)},\ \widehat{\theta}^*_{(1-\gamma/2)}\right).$$

BCa CI for $\psi \in \{\alpha, \theta\}$:
Compute the bias-correction constant

$$z_{0,\psi} = \Phi^{-1}\left[\frac{1}{K}\sum_{k=1}^{K} I\left(\widehat{\psi}^{*(k)} < \widehat{\psi}\right)\right].$$

Obtain the jackknife estimates $\widehat{\psi}_{(-1)}, \ldots, \widehat{\psi}_{(-n)}$ by successively deleting one observation from the original sample, and compute

$$\bar{\psi}_{(\cdot)} = \frac{1}{n}\sum_{i=1}^{n}\widehat{\psi}_{(-i)}.$$

Then compute the acceleration constant

$$a_\psi = \frac{\sum_{i=1}^{n}\left(\bar{\psi}_{(\cdot)} - \widehat{\psi}_{(-i)}\right)^3}{6\left[\sum_{i=1}^{n}\left(\bar{\psi}_{(\cdot)} - \widehat{\psi}_{(-i)}\right)^2\right]^{3/2}}.$$

Compute

$$q_{L,\psi} = \Phi\left[z_{0,\psi} + \frac{z_{0,\psi} + z_{\gamma/2}}{1 - a_\psi(z_{0,\psi} + z_{\gamma/2})}\right],$$

and

$$q_{U,\psi} = \Phi\left[z_{0,\psi} + \frac{z_{0,\psi} + z_{1-\gamma/2}}{1 - a_\psi(z_{0,\psi} + z_{1-\gamma/2})}\right].$$

The BCa confidence interval is

$$\left(\widehat{\psi}^*_{(q_{L,\psi})}, \widehat{\psi}^*_{(q_{U,\psi})}\right).$$

Thus, the BCa intervals for α and θ are

$$\left(\widehat{\alpha}^*_{(q_{L,\alpha})}, \widehat{\alpha}^*_{(q_{U,\alpha})}\right), \qquad \left(\widehat{\theta}^*_{(q_{L,\theta})}, \widehat{\theta}^*_{(q_{U,\theta})}\right).$$

S5.3. Bayesian estimation of the EQL model

As a complementary inferential approach, we also consider Bayesian estimation for the EQL parameters. Independent Gamma prior distributions are assigned to α and θ, and posterior inference is performed using a Metropolis-within-Gibbs algorithm. Let $X_1, X_2, \ldots, X_n$ be a random sample from the EQL distribution. For the observed sample $\mathbf{x} = (x_1, \ldots, x_n)$, the likelihood function is

$$L(\alpha, \theta \mid \mathbf{x}) = \prod_{i=1}^{n} \frac{\alpha\theta(1+\theta^2 x_i)}{1+\theta} e^{-\theta x_i} [\mathcal{G}(x_i;\theta)]^{\alpha-1}.$$

Ignoring terms that do not depend on (α, θ), the likelihood can be written as

$$L(\alpha, \theta \mid \mathbf{x}) \propto \alpha^n \theta^n (1+\theta)^{-n} \exp\left(-\theta \sum_{i=1}^{n} x_i\right) \prod_{i=1}^{n} (1+\theta^2 x_i) \prod_{i=1}^{n} [\mathcal{G}(x_i;\theta)]^{\alpha-1}. \tag{S5.3}$$

We assume that α and θ are a priori independent and follow Gamma distributions parameterized in terms of their shape and rate parameters: $\alpha \sim \text{Gamma}(a_1, b_1)$, and $\theta \sim \text{Gamma}(a_2, b_2)$, where $a_j > 0$ and $b_j > 0$, $j = 1, 2$. Hence, the joint prior density is

$$\pi(\alpha, \theta) = \pi_1(\alpha)\pi_2(\theta) \propto \alpha^{a_1-1} \theta^{a_2-1} \exp(-b_1\alpha - b_2\theta), \qquad \alpha, \theta > 0. \tag{S5.4}$$

Combining Eqs (S5.3) and (S5.4), the joint posterior density is given, up to a normalizing constant, by

$$\pi(\alpha, \theta \mid \mathbf{x}) \propto \alpha^{n+a_1-1} \theta^{n+a_2-1} (1+\theta)^{-n} \prod_{i=1}^{n} (1+\theta^2 x_i) \exp\left[-\theta\left(b_2 + \sum_{i=1}^{n} x_i\right) - b_1\alpha\right] \prod_{i=1}^{n} [\mathcal{G}(x_i;\theta)]^{\alpha-1}.$$

S5.3.1. Full conditional distribution of α

Conditioning on θ and $\mathbf{x}$, the terms in Eq (S5.3) that depend on α give

$$\pi(\alpha \mid \theta, \mathbf{x}) \propto \alpha^{n+a_1-1} \exp(-b_1\alpha) \prod_{i=1}^{n} [\mathcal{G}(x_i;\theta)]^{\alpha-1}.$$

Since

$$\prod_{i=1}^{n} [\mathcal{G}(x_i;\theta)]^{\alpha-1} = \exp\left\{(\alpha-1) \sum_{i=1}^{n} \log[\mathcal{G}(x_i;\theta)]\right\},$$

the conditional posterior can be expressed as

$$\pi(\alpha \mid \theta, \mathbf{x}) \propto \alpha^{n+a_1-1} \exp\left\{-\alpha\left[b_1 - \sum_{i=1}^{n} \log[\mathcal{G}(x_i;\theta)]\right]\right\}.$$

Therefore, under the shape–rate parameterization,

$$\alpha \mid \theta, \mathbf{x} \sim \text{Gamma}\left(n + a_1,\ b_1 - \sum_{i=1}^{n} \log[\mathcal{G}(x_i;\theta)]\right). \tag{S5.5}$$

Notice that $0 < \mathcal{G}(x_i;\theta) < 1$ for $x_i > 0$ and $\theta > 0$, so that $\log[\mathcal{G}(x_i;\theta)] < 0$. Consequently, the rate parameter in Eq (S5.5) is positive for $a_1, b_1 > 0$.

S5.3.2. Full conditional distribution of θ

Conditioning on α and $\mathbf{x}$, the full conditional distribution of θ is

$$\pi(\theta \mid \alpha, \mathbf{x}) \propto \theta^{n+a_2-1}(1+\theta)^{-n} \prod_{i=1}^{n}(1+\theta^2 x_i) \exp\left[-\theta\left(b_2 + \sum_{i=1}^{n} x_i\right)\right] \prod_{i=1}^{n}[\mathcal{G}(x_i;\theta)]^{\alpha-1}, \qquad \theta > 0. \quad \text{(S5.6)}$$

Unlike the conditional distribution of α, the density in Eq (S5.6) does not correspond to a standard distributional family. Therefore, a Metropolis–Hastings step is used to generate samples from this conditional distribution.

S5.3.3. Metropolis-within-Gibbs algorithm

The posterior samples are generated using a Metropolis-within-Gibbs scheme. At each iteration, α is first sampled directly from its Gamma full conditional distribution in Eq (S5.5). Subsequently, θ is updated using a Metropolis–Hastings step based on its full conditional distribution in Eq (S5.6). Because $\theta > 0$, a logarithmic transformation is employed. Let

$$\phi = \log(\theta), \qquad \theta = e^{\phi}.$$

A normal random-walk proposal is then generated according to

$$\phi^* = \phi^{(t-1)} + \epsilon_t, \qquad \epsilon_t \sim N(0, \sigma_\theta^2),$$

and the proposed value on the original scale is

$$\theta^* = \exp(\phi^*).$$

The transformation requires the Jacobian

$$\left|\frac{d\theta}{d\phi}\right| = \theta.$$

Consequently, the Metropolis–Hastings acceptance ratio is

$$r_\theta = \frac{\pi(\alpha^{(t)}, \theta^* \mid \mathbf{x})\theta^*}{\pi(\alpha^{(t)}, \theta^{(t-1)} \mid \mathbf{x})\theta^{(t-1)}}.$$

The proposed value θ^* is accepted with probability

$$p_\theta = \min\{1, r_\theta\}.$$

If the proposal is rejected, we set $\theta^{(t)} = \theta^{(t-1)}$. The proposal standard deviation σ_θ can be adapted during the burn-in period to obtain an adequate acceptance rate. After discarding the burn-in iterations, the retained posterior samples are used to compute Bayesian point estimates and credible intervals. The complete procedure is summarized in Algorithm 3.

Algorithm 3. Metropolis-within-Gibbs algorithm for Bayesian inference of the EQL model.

Input: Data $\mathbf{x} = (x_1, \ldots, x_n)$, hyperparameters (a_1, b_1, a_2, b_2), total number of iterations N, burn-in period B, and proposal standard deviation σ_θ.
Initialize: $\alpha^{(0)} > 0$ and $\theta^{(0)} > 0$
for $t = 1, \ldots, N$ **do**
    Gibbs update for α
    Compute

$$b_\alpha^{(t)} = b_1 - \sum_{i=1}^{n} \log[\mathcal{G}(x_i; \theta^{(t-1)})].$$

    Generate

$$\alpha^{(t)} \sim \text{Gamma}\left(n + a_1, b_\alpha^{(t)}\right).$$

    Metropolis–Hastings update for θ
    Generate

$$\phi^* = \log(\theta^{(t-1)}) + \epsilon_t, \qquad \epsilon_t \sim N(0, \sigma_\theta^2).$$

    Set

$$\theta^* = \exp(\phi^*).$$

    Compute

$$r_\theta = \frac{\pi(\alpha^{(t)}, \theta^* \mid \mathbf{x})\theta^*}{\pi(\alpha^{(t)}, \theta^{(t-1)} \mid \mathbf{x})\theta^{(t-1)}}.$$

    Generate $u \sim U(0, 1)$.
    if $u \le \min(1, r_\theta)$ **then**
        Set $\theta^{(t)} = \theta^*$.
    else
        Set $\theta^{(t)} = \theta^{(t-1)}$.
    end if
    if $t \le B$ **then**
        Adapt σ_θ according to the desired acceptance rate.
    end if
end for
Discard the first B iterations.
Compute posterior means:

$$\widehat{\alpha}_{\text{Bayes}} = \frac{1}{N-B} \sum_{t=B+1}^{N} \alpha^{(t)}, \qquad \widehat{\theta}_{\text{Bayes}} = \frac{1}{N-B} \sum_{t=B+1}^{N} \theta^{(t)}.$$

Return: Posterior samples, Bayesian point estimates, credible intervals, and convergence diagnostics.

S6. Additional results on applications

This supplementary material provides additional numerical and graphical results for the four real-life applications considered in the manuscript. The analyses presented here complement the results reported in the main text and include additional goodness-of-fit diagnostics, alternative estimation methods, bootstrap confidence intervals, and Bayesian diagnostics.

S6.1. Additional diagnostic plots

To provide additional graphical information on the empirical characteristics of the four datasets, we report several distribution-free diagnostic plots in Figures S4–S7, including boxplots, histograms, scatter plots, violin plots, strip plots, and nonparametric density estimates. These plots complement the descriptive statistics and fitted-model analyses presented in the main manuscript and provide a more detailed visualization of the distributional features of the datasets.

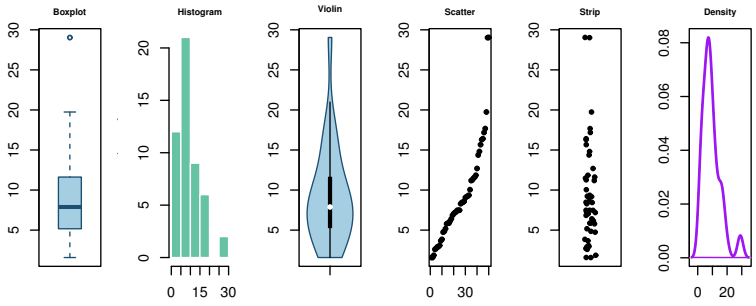


Figure S4. Distribution-free diagnostic plots for Dataset I.

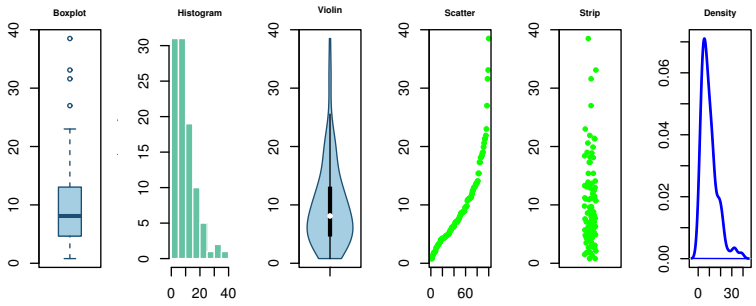


Figure S5. Distribution-free diagnostic plots for Dataset II.

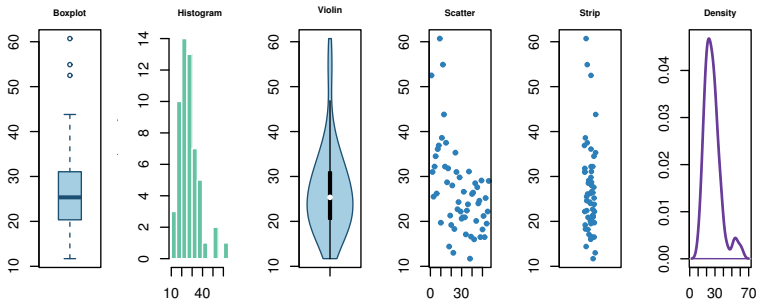


Figure S6. Distribution-free diagnostic plots for Dataset III.

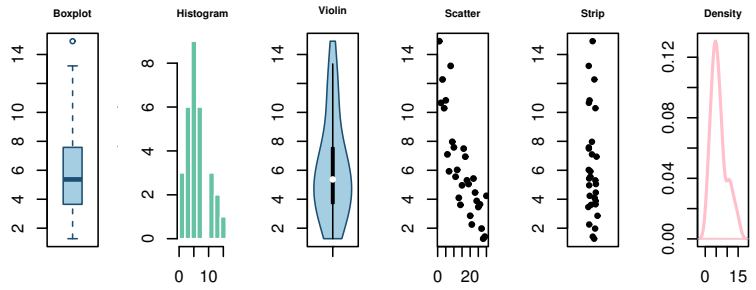


Figure S7. Distribution-free diagnostic plots for Dataset IV.

S6.2. Complete maximum likelihood estimates

This section reports the complete maximum likelihood estimates and their corresponding standard errors for all competing distributions considered in the four real-data applications.

Tables S6 and S7 show the complete maximum likelihood (ML) results for all distributions fitted to the four datasets. Each table gives the ML estimates with standard errors (in parentheses), the negative log-likelihood ($-\hat{\ell}$), AIC, BIC, and the KS and CvM statistics with their p-values. Table S6 covers Datasets I and II, and Table S7 covers Datasets III and IV. The EQL model, shown in bold, has the best overall fit. It is best on all criteria for Datasets II and III, and on all criteria except BIC for Dataset I. For Dataset IV it has the largest likelihood and the smallest CvM statistic, while the one-parameter Garphy model has slightly smaller AIC and BIC.

Table S6. Summary of maximum likelihood estimates (SE in parentheses) and model selection criteria for Datasets I and II.

Model	Parameter Estimates (SE)	$-\hat{\ell}$	AIC	BIC	KS	p-value	CvM	p-value
		Dataset I						
EQL$_{(\hat{\alpha},\hat{\theta})}$	2.6876(0.57796), 0.2203(0.03444)	151.9815	307.9630	311.7871	0.06325	0.98080	0.03123	0.97314
PL$_{(\hat{\alpha},\hat{\beta})}$	1.1988(0.11004), 0.1251(0.03490)	152.7449	309.4898	313.3139	0.08284	0.85447	0.03926	0.93862
Weibull$_{(k,\lambda)}$	1.6292(0.17194), 10.4049(0.95546)	153.0918	310.1835	314.0076	0.09151	0.76218	0.05224	0.86472
XGamma$_{(\theta)}$	0.2811(0.02434)	154.7419	311.4837	313.3957	0.09058	0.77280	0.08739	0.65229
ER$_{(\hat{\alpha},\hat{\theta})}$	0.7617(0.13731), 0.00675(0.00138)	154.0178	312.0357	315.8597	0.11946	0.43940	0.09903	0.59148
XL$_{(\theta)}$	0.1845(0.01867)	155.8850	313.7701	315.6821	0.13420	0.30124	0.19920	0.26948
MWE$_{(\hat{\alpha},\hat{\theta})}$	2.7423(1.67142), 0.1269(0.01772)	156.0086	316.0171	319.8412	0.14884	0.19712	0.23669	0.20654
Garphy$_{(\theta)}$	0.36320(0.02629)	153.6555	309.3111	311.2232	0.07908	0.8888	0.04675	0.89770
SBH$_{(\eta)}$	0.2520(0.02250)	157.0556	316.1113	318.0233	0.13294	0.31169	0.23078	0.21521
NH$_{(\hat{\alpha},\hat{\lambda})}$	8.5031(0.000002), 0.00821(0.00075)	156.7630	317.5260	321.3500	0.12325	0.40074	0.19445	0.27900
IK$_{(\hat{\alpha},\hat{\beta})}$	1.6900(0.18729), 22.5777(7.65679)	156.8358	317.6716	321.4956	0.14404	0.22769	0.20906	0.25097
ZL$_{(\theta)}$	0.1583(0.01920)	158.9145	319.8290	321.7410	0.18146	0.06515	0.43895	0.05673
Q-L$_{(\theta)}$	0.1210(0.01880)	161.1552	324.3104	326.2224	0.20571	0.02476	0.61267	0.02043
Obulezi$_{(\lambda)}$	0.10855(0.01553)	161.3205	324.6411	326.5531	0.20425	0.02633	0.60677	0.02113
		Dataset II						
EQL$_{(\hat{\alpha},\hat{\theta})}$	2.11497(0.31014), 0.17962(0.02101)	317.1524	638.3049	643.5152	0.04157	0.99522	0.02401	0.99180
PL$_{(\hat{\alpha},\hat{\beta})}$	1.08319(0.07042), 0.15298(0.02818)	318.3186	640.6372	645.8475	0.05200	0.94968	0.04578	0.90236
Weibull$_{(k,\lambda)}$	1.45849(0.10979), 10.95532(0.79424)	318.7307	641.4614	646.6717	0.05780	0.89206	0.06104	0.80858
XL$_{(\theta)}$	0.17443(0.01247)	320.7617	643.5234	646.1286	0.09050	0.38584	0.12536	0.47492
XGamma$_{(\theta)}$	0.26341(0.01616)	321.0203	644.0405	646.6457	0.06249	0.82968	0.08396	0.67035
MWE$_{(\hat{\alpha},\hat{\theta})}$	3.06560(1.56049), 0.11862(0.01208)	320.6070	645.2139	650.4242	0.10050	0.26471	0.16801	0.33946
ER$_{(\hat{\alpha},\hat{\theta})}$	0.62954(0.07771), 0.00482(0.00073)	321.5182	647.0364	652.2467	0.09450	0.33367	0.20431	0.25949
Garphy$_{(\theta)}$	0.30347(0.01747)	322.4647	646.9294	649.5346	0.11330	0.15339	0.28559	0.14845
SBH$_{(\eta)}$	0.23712(0.01498)	323.4226	648.8451	651.4503	0.09879	0.28326	0.17947	0.31138
NH$_{(\hat{\alpha},\hat{\lambda})}$	3.41654(2.05882), 0.02057(0.01476)	323.4486	650.8971	656.1074	0.10662	0.20564	0.20862	0.25156
ZL$_{(\theta)}$	0.14806(0.01274)	325.2583	652.5167	655.1219	0.14426	0.03114	0.43754	0.05741
Q-L$_{(\theta)}$	0.11241(0.01226)	328.7856	659.5712	662.1764	0.17316	0.00497	0.71632	0.01146
Obulezi$_{(\lambda)}$	0.10177(0.01028)	329.0203	660.0405	662.6457	0.17301	0.00502	0.71539	0.01152
IK$_{(\hat{\alpha},\hat{\beta})}$	1.45017(0.11549), 13.62880(2.87723)	328.7421	661.4842	666.6946	0.09114	0.37718	0.28186	0.15216

Table S7. Summary of maximum likelihood estimates (SE in parentheses) and model selection criteria for Datasets III and IV.

Model	Parameter Estimates (SE)	$-\hat{\ell}$	AIC	BIC	KS	p-value	CvM	p-value
			Dataset III					
EQL$_{(\hat{\alpha},\hat{\theta})}$	19.12605(6.19660), 0.14779(0.01737)	199.5874	403.1749	407.2256	0.05527	0.99553	0.01458	0.99975
PL$_{(\hat{\alpha},\hat{\beta})}$	2.01065(0.18478), 0.00235(0.00153)	203.7071	411.4142	415.4649	0.10159	0.60999	0.11147	0.53298
Weibull$_{(k,\lambda)}$	2.80991(0.26310), 30.12801(1.52253)	206.4170	416.8340	420.8847	0.12097	0.38550	0.18830	0.29183
XGamma$_{(\theta)}$	0.10678(0.00835)	217.0067	436.0134	438.0388	0.24680	0.00218	0.87642	0.00461
ER$_{(\hat{\alpha},\hat{\theta})}$	2.73401(0.61282), 0.00218(0.00032)	202.3168	408.6336	412.6843	0.08245	0.84103	0.07763	0.70762
XL$_{(\theta)}$	0.06968(0.00660)	225.1234	452.2469	454.2722	0.29895	0.00009	1.34154	0.00035
MWE$_{(\hat{\alpha},\hat{\theta})}$	2.19934(0.86288), 0.04385(0.00556)	230.5294	465.0587	469.1094	0.32880	0.00001	1.65820	0.00006
Garphy$_{(\theta)}$	0.11163(0.00861)	213.1424	428.2848	430.3101	0.21217	0.00129	0.65442	0.01611
SBH$_{(\eta)}$	0.10222(0.00809)	220.4541	442.9082	444.9335	0.27473	0.00043	1.08771	0.00143
NH$_{(\hat{\alpha},\hat{\lambda})}$	9.05158(5.25756), 0.003108(0.001906)	227.3866	458.7732	462.8239	0.37045	< 0.0001	2.10696	< 0.0001
IK$_{(\hat{\alpha},\hat{\beta})}$	1.29079(0.09079), 22.32190(13.36287)	230.6057	465.2114	469.2621	0.28135	0.00028	1.38904	0.00027
ZL$_{(\theta)}$	0.05792(0.00660)	234.7318	471.4635	473.4889	0.37722	< 0.0001	2.17930	< 0.0001
Q-L$_{(\theta)}$	0.03870(0.00537)	240.2616	482.5231	484.5485	0.39559	< 0.0001	2.42207	< 0.0001
Obulezi$_{(\lambda)}$	0.03724(0.00498)	240.2958	482.5917	484.6170	0.39512	< 0.0001	2.41610	< 0.0001
			Dataset IV					
EQL$_{(\hat{\alpha},\hat{\theta})}$	3.23764(0.89824), 0.38713(0.07218)	76.69359	157.3872	160.1896	0.07817	0.98615	0.02261	0.99464
PL$_{(\hat{\alpha},\hat{\beta})}$	1.37745(0.16486), 0.14207(0.04935)	77.00929	158.0186	160.8210	0.09185	0.94183	0.03808	0.94555
Weibull$_{(k,\lambda)}$	1.87999(0.26292), 6.96371(0.71499)	77.03425	158.0685	160.8709	0.09999	0.89616	0.04613	0.90271
ER$_{(\hat{\alpha},\hat{\theta})}$	0.94632(0.22630), 0.01930(0.00473)	77.10839	158.2168	161.0192	0.11057	0.81799	0.05819	0.82917
XGamma$_{(\theta)}$	0.40661(0.04621)	79.99086	161.9817	163.3829	0.17126	0.30633	0.15820	0.36704
IK$_{(\hat{\alpha},\hat{\beta})}$	1.99922(0.28493), 23.55698(10.39502)	79.64320	163.2864	166.0888	0.12976	0.64627	0.09531	0.61155
NH$_{(\hat{\alpha},\hat{\lambda})}$	23.85352(8.2146), 0.004518(0.00168)	79.93941	163.8788	166.6812	0.19436	0.18141	0.21423	0.24207
XL$_{(\theta)}$	0.26316(0.03472)	81.26130	164.5226	165.9238	0.20154	0.15202	0.24163	0.19970
MWE$_{(\hat{\alpha},\hat{\theta})}$	2.53831(1.78786), 0.19142(0.03394)	80.80980	165.6196	168.4220	0.19918	0.16124	0.22713	0.22094
Garphy$_{(\theta)}$	0.54406(0.03040)	77.34498	156.6900	158.0912	0.07727	0.98981	0.02516	0.99037
SBH$_{(\eta)}$	0.35272(0.04172)	82.33590	166.6718	168.0730	0.22139	0.09005	0.31896	0.11930
ZL$_{(\theta)}$	0.23411(0.03650)	82.95928	167.9186	169.3198	0.24259	0.04868	0.39745	0.07277
Q-L$_{(\theta)}$	0.19455(0.04049)	84.25645	170.5129	171.9141	0.26741	0.02200	0.51732	0.03529
Obulezi$_{(\lambda)}$	0.16469(0.00309)	84.52338	171.0468	172.4480	0.26344	0.02511	0.50064	0.03897

S6.3. Additional goodness-of-fit diagnostics

Additional graphical goodness-of-fit diagnostics for the EQL model are presented in Figures S8–S11. For each dataset, the empirical and fitted distributions are compared using quantile-quantile (QQ) plots, probability-probability (PP) plots, fitted cumulative distribution functions, and fitted survival functions. These plots provide additional visual evidence of the adequacy of the EQL distribution and complement the numerical goodness-of-fit results reported in the main manuscript.

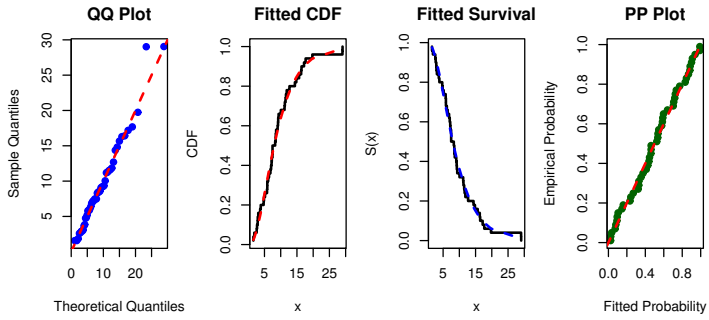


Figure S8. Additional goodness-of-fit diagnostics for the EQL model fitted to Dataset I.

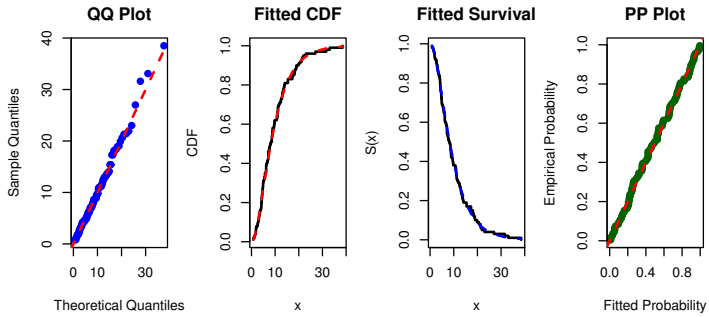


Figure S9. Additional goodness-of-fit diagnostics for the EQL model fitted to Dataset II.

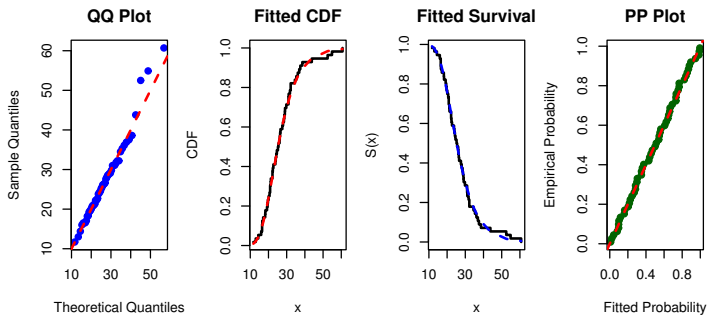


Figure S10. Additional goodness-of-fit diagnostics for the EQL model fitted to Dataset III.

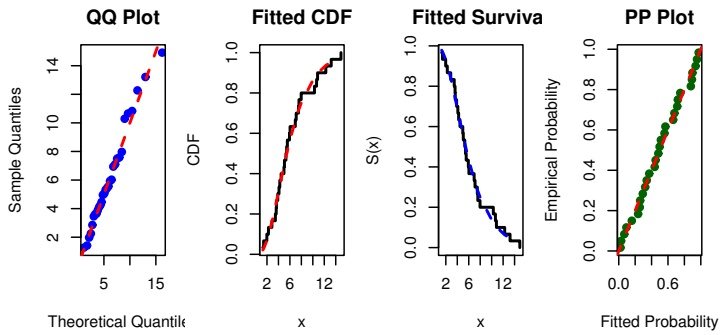


Figure S11. Additional goodness-of-fit diagnostics for the EQL model fitted to Dataset IV.

S6.4. Profile likelihood and contour plots

To further examine the numerical behavior of the likelihood function, Figure S12 presents the profile log-likelihood and contour plots for the parameters α and θ of the EQL distribution for the four datasets. The profile likelihood curves provide a graphical assessment of the local behavior of the likelihood around the maximum likelihood estimates, while the contour plots illustrate the corresponding joint likelihood surface.

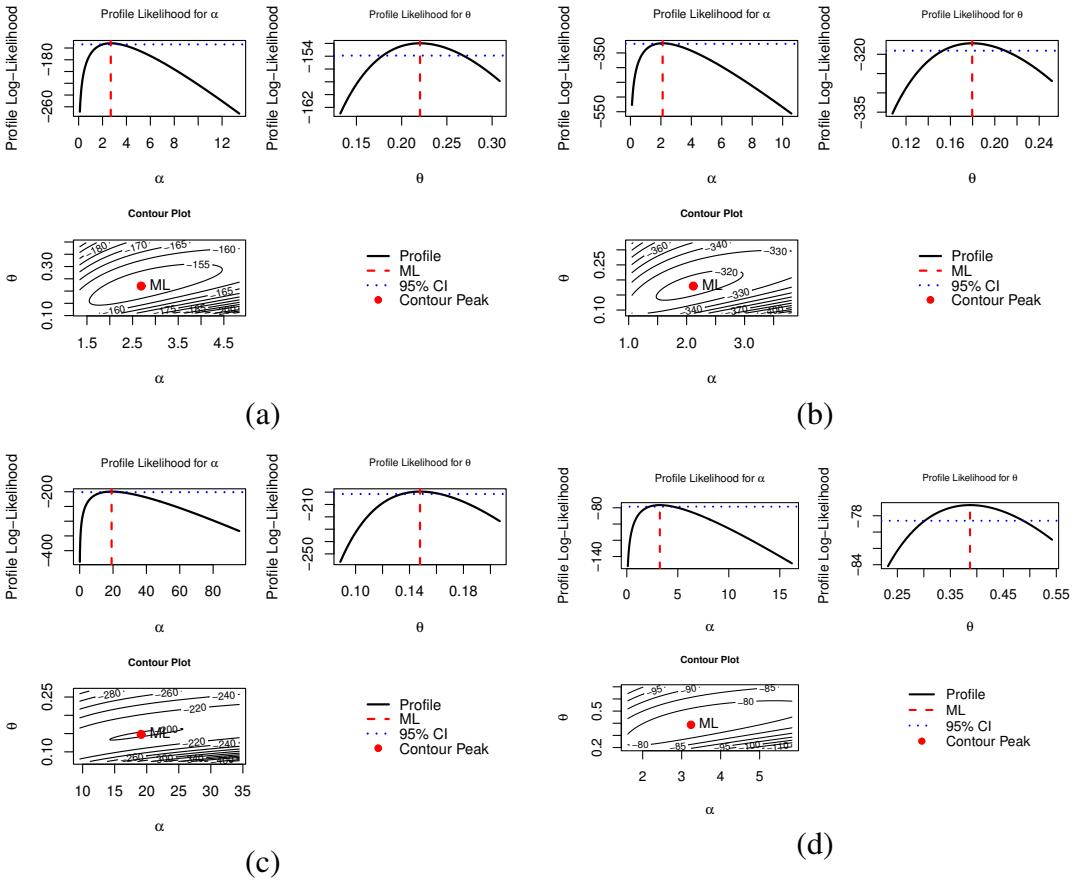


Figure S12. Profile log-likelihood and contour plots for the parameters α and θ of the EQL model for (a) Dataset I, (b) Dataset II, (c) Dataset III, and (d) Dataset IV.

S6.5. Alternative estimation methods

In addition to maximum likelihood estimation, the EQL distribution was fitted using several alternative estimation procedures, including maximum product of spacings (MPS), Anderson–Darling (AD), minimum spacing absolute distance (MSAD), ordinary least squares (OLS), weighted least squares (WLS), and Cramér–von Mises (CvM) estimation. Table S8 reports the resulting parameter estimates together with the Kolmogorov–Smirnov (KS) and Cramér–von Mises (CvM) goodness-of-fit statistics and their corresponding p-values. Overall, the alternative estimation methods produce parameter estimates that are broadly consistent with those obtained by maximum likelihood. The corresponding goodness-of-fit statistics indicate that several of these methods provide

satisfactory fits across the four datasets.

Table S8. Parameter estimates and goodness-of-fit statistics for the EQL model under alternative estimation methods.

	Dataset I						Dataset II					
Stat.	MPS	AD	MSAD	OLS	WLS	CvM	MPS	AD	MSAD	OLS	WLS	CvM
$\widehat{\alpha}$	2.36690	2.61280	3.04217	2.63590	2.50767	2.82248	2.10321	2.06913	2.06747	2.01156	2.01673	2.06941
$\widehat{\theta}$	0.20104	0.21721	0.23597	0.21772	0.21109	0.22779	0.12031	0.17857	0.18018	0.17593	0.17514	0.17981
KS	0.07131	0.06633	0.07176	0.06411	0.06940	0.06118	0.09267	0.03827	0.04086	0.04349	0.04149	0.04003
p-value	0.94529	0.96996	0.94264	0.97809	0.95583	0.98632	0.97892	0.99855	0.99619	0.99150	0.99532	0.99715
CvM	0.04082	0.03229	0.03317	0.03189	0.03472	0.03047	0.06272	0.02058	0.02009	0.02066	0.02120	0.02000
p-value	0.93063	0.96930	0.96594	0.97075	0.95960	0.97568	0.95292	0.99658	0.99705	0.99649	0.99591	0.99714
	Dataset III						Dataset IV					
Stat.	MPS	AD	MSAD	OLS	WLS	CvM	MPS	AD	MSAD	OLS	WLS	CvM
$\widehat{\alpha}$	15.2162	19.5995	19.58936	19.06826	18.5072	20.84029	2.66293	3.04971	3.46573	2.92669	2.76107	3.28387
$\widehat{\theta}$	0.1366	0.14967	0.14943	0.148508	0.14713	0.15271	0.34035	0.37208	0.40382	0.36405	0.34853	0.39187
KS	0.07218	0.04972	0.05091	0.05064	0.05224	0.04528	0.08991	0.07507	0.08563	0.08128	0.08574	0.08091
p-value	0.9323	0.99908	0.99865	0.99876	0.99799	0.99984	0.95057	0.99109	0.96690	0.97949	0.96654	0.98037
CvM	0.02973	0.01279	0.01298	0.01334	0.01423	0.01225	0.03105	0.02370	0.02303	0.02494	0.02841	0.02250
p-value	0.9780	0.99992	0.99991	0.99989	0.99980	0.99995	0.97449	0.99299	0.99403	0.99080	0.98264	0.99478

S6.6. Bootstrap confidence intervals

To further investigate the uncertainty associated with the maximum likelihood estimates, four bootstrap-based confidence interval procedures were considered: Normal, Basic, Percentile, and bias-corrected and accelerated (BCa) intervals. Table S9 reports the resulting 95% confidence intervals for α and θ across the four datasets. For some datasets, the Normal and Basic procedures produce negative lower bounds for α, which are incompatible with the parameter space $\alpha > 0$. For some datasets, the Normal and Basic procedures produce negative lower bounds for α, despite the restriction $\alpha > 0$. In contrast, the Percentile and BCa intervals reported in Table S9 remain entirely within the admissible parameter space. This illustrates the practical advantage of bootstrap intervals that respect the empirical shape of the sampling distribution in these applications.

Table S9. Bootstrap-based 95% confidence intervals for the parameters α and θ across the four datasets.

	Dataset I		Dataset II	
Method	α	θ	α	θ
Normal CI	(1.297, 3.741)	(0.1440, 0.2813)	(1.430, 2.670)	(0.1329, 0.2188)
Basic CI	(1.037, 3.442)	(0.1363, 0.2745)	(1.325, 2.570)	(0.1294, 0.2142)
Percentile CI	(1.933, 4.338)	(0.1662, 0.3044)	(1.660, 2.905)	(0.1450, 0.2299)
BCa CI	(1.814, 3.921)	(0.1554, 0.2858)	(1.582, 2.744)	(0.1387, 0.2212)
	Dataset III		Dataset IV	
Normal CI	(-0.48, 33.25)	(0.1063, 0.1818)	(0.572, 5.121)	(0.2232, 0.5117)
Basic CI	(-5.32, 26.97)	(0.1030, 0.1782)	(-0.033, 4.277)	(0.1953, 0.4837)
Percentile CI	(11.29, 43.58)	(0.1174, 0.1926)	(2.198, 6.508)	(0.2906, 0.5790)
BCa CI	(10.15, 36.81)	(0.1120, 0.1833)	(1.978, 5.345)	(0.2715, 0.5296)

S6.7. Bayesian convergence and posterior diagnostics

Additional graphical diagnostics were performed to assess the convergence and mixing of the MCMC algorithms used for Bayesian inference. Figure S13 displays the joint posterior contours for α and θ. These plots provide additional information about the dependence structure between the two parameters and the concentration of the posterior distribution. The trace plots show no apparent trends or prolonged departures from the main regions of posterior mass. The Gelman–Rubin diagnostics reported in Figures S14–S17 provide additional evidence of convergence, with the corresponding $\widehat{R}$ values close to one.

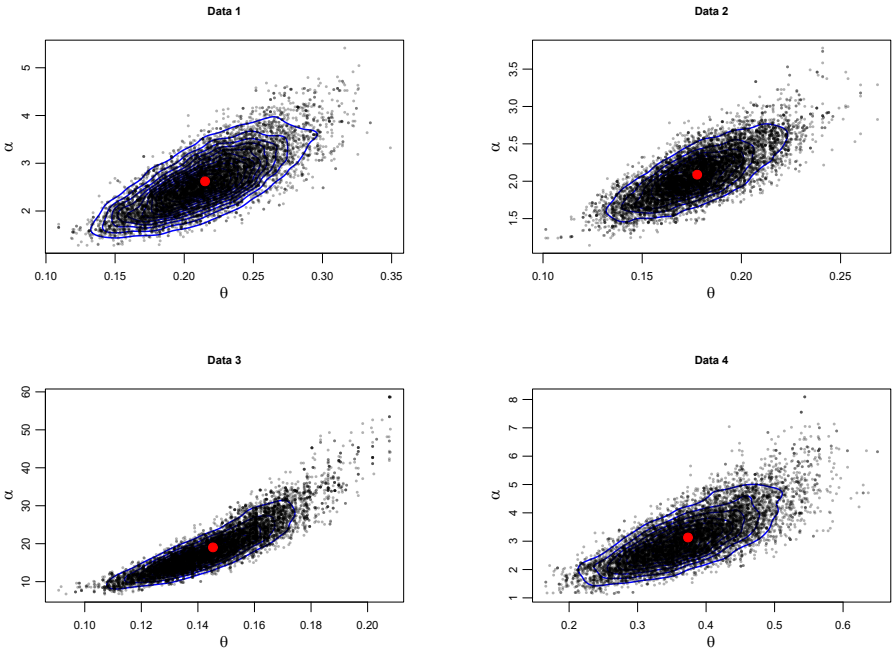


Figure S13. Joint posterior contour plots for α and θ for the four datasets.

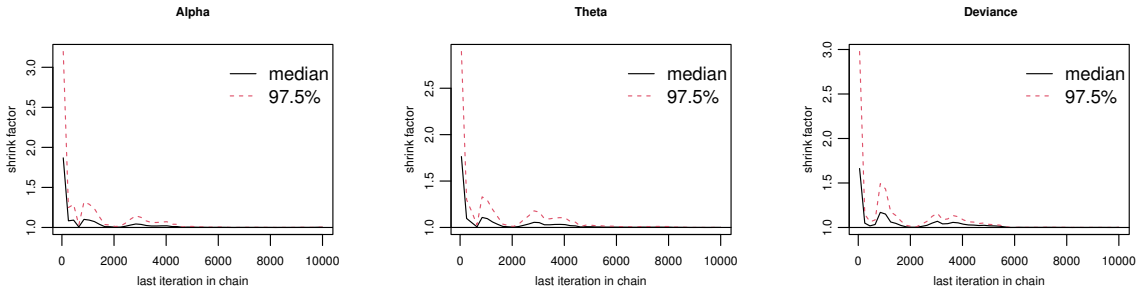


Figure S14. Gelman–Rubin convergence diagnostics for Dataset I.

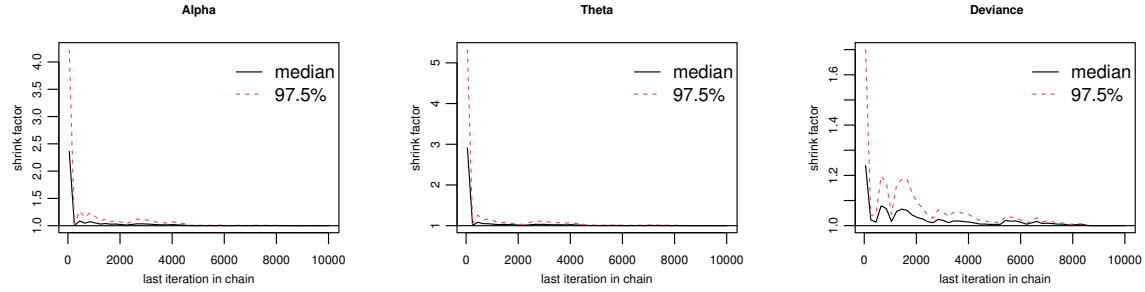


Figure S15. Gelman–Rubin convergence diagnostics for Dataset II.

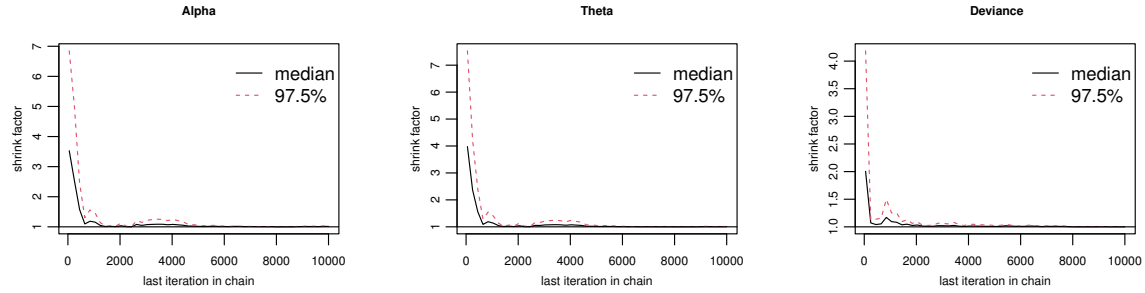


Figure S16. Gelman–Rubin convergence diagnostics for Dataset III.

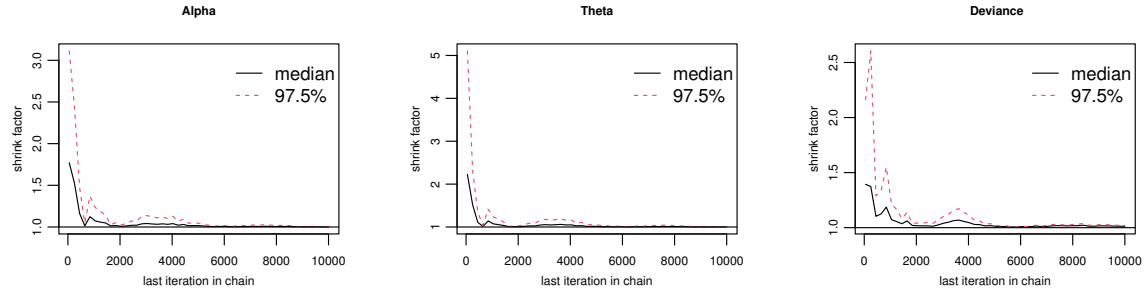


Figure S17. Gelman–Rubin convergence diagnostics for Dataset IV.

The posterior and convergence diagnostics provide additional information on the numerical behavior of the Bayesian analysis. The trace plots show stable chains, the posterior densities are well concentrated, and the Gelman–Rubin diagnostics indicate satisfactory convergence across the four datasets.

References

1. U. Kamps, *A concept of generalized order statistics*, Stuttgart: Teubner, 1995. http://dx.doi.org/10.1007/978-3-663-09196-7

2. S. Hussain, P. J. Hazarika, I. Sadok, M. F. Abouelenein, M. S. Eliwa, The unit-exponentiated Z-Lindley distribution: mathematical theory, statistical inference, and empirical applications, *Math. Sci.,* 2026. http://dx.doi.org/10.57647/p85005.0184.mathsci

3. H. Torabi, A new method for hypotheses testing using spacings, *Statist. Probab. Lett.,* **76** (2006), 1345–1347. http://dx.doi.org/10.1016/j.spl.2006.02.003



AIMS Press

© 2026 the Author(s), licensee AIMS Press. This is an open access article distributed under the terms of the Creative Commons Attribution License (https://creativecommons.org/licenses/by/4.0)